Intrinsic Spin-Orbit Torque Arising from the Berry Curvature in a Metallic-Magnet/Cu-Oxide Interface

Tenghua Gao,[1] Alireza Qaiumzadeh,[2,3] Hongyu An,[1] Akira Musha,[1] Yuito Kageyama,[1] Ji Shi,[4] and Kazuya Ando[1,*]
[1]Department of Applied Physics and Physico-Informatics, Keio University, Yokohama 223-8522, Japan
[2]Center for Quantum Spintronics, Department of Physics, Norwegian University of Science and Technology, NO-7491 Trondheim, Norway
[3]Department of Physics, Institute for Advanced Studies in Basic Sciences (IASBS), Zanjan 45137-66731, Iran
[4]School of Materials and Chemical Technology, Tokyo Institute of Technology, Tokyo 152-8552, Japan

(Received 26 November 2017; revised manuscript received 18 May 2018; published 6 July 2018)

We report the observation of the intrinsic dampinglike spin-orbit torque (SOT) arising from the Berry curvature in metallic-magnet/CuO_x heterostructures. We show that a robust dampinglike SOT, an order of magnitude larger than a fieldlike SOT, is generated in the heterostructure despite the absence of the bulk spin-orbit effect in the CuO_x layer. Furthermore, by tuning the interfacial oxidation level, we demonstrate that the fieldlike SOT changes drastically and even switches its sign, which originates from oxygen-modulated spin-dependent disorder. These results provide important information for a fundamental understanding of the physics of the SOTs.

DOI: 10.1103/PhysRevLett.121.017202

The emergence of the exciting field of spin orbitronics [1,2] requires the fundamental understanding of spin-orbit torques (SOTs), which trigger magnetic dynamics via the transfer of angular momentum from an atomic lattice to local magnetization through carriers [3–6]. The SOTs, dampinglike (DL) and fieldlike (FL) torques, can arise from both bulk and interfacial relativistic spin-orbit interactions (SOIs). In a ferromagnetic-metal (FM)–heavy-metal (HM) heterostructure, a spin current is generated from spin-dependent scattering due to the bulk SOI in the HM, which is known as the spin Hall effect (SHE) [7–11]. This spin current can exert a larger DL torque relative to a FL torque through the spin-transfer mechanism [12–14]. The other source for the SOTs is the Rashba-Edelstein effect due to the interfacial SOI [15–18], which refers to the creation of nonequilibrium spin polarization at the HM/FM interface with broken inversion symmetry. Although the Rashba-Edelstein effect primarily generates a large FL torque through spin exchange coupling, recent theoretical studies predict that a comparable DL torque in magnitude as a FL torque can be generated by taking into account spin-dependent scattering in a three-dimensional model of the interfacial SOI [19–21]. Moreover, the theory and experiment demonstrate that the intrinsic mechanism of the SOT generation with the Berry-curvature origin can produce a sizable DL component in a diluted magnetic semiconductor (DMS) [6,22], and the existence of this intrinsic SOT is also expected in metallic bilayers, such as a Pt/Co bilayer [22–25]. Since the SOTs generated from all the contributions above have the same symmetry, it is a great experimental challenge to distinguish the mechanisms, consequently hindering the efficient engineering of the SOTs.

A promising system for studying the current-induced spin-orbit effect purely arising from the interfacial SOI is FM/insulating-oxide heterostructures, where the bulk spin-orbit effect can be neglected due to the insulating nature. Among the various oxides, Cu oxides (Cu_2O and CuO) have been intensively studied in a wide range of fields due to its abundant physical properties, such as ferromagnetism in a ZnO-based DMS [26–28] and commensurate antiferromagnetic order at a low temperature [29–31]. Furthermore, a recent study has demonstrated that Cu becomes an efficient SOT generator through oxidation, even though nonoxidized Cu possesses weak SOI [32]. Efficient SOT generation, combined with the great flexibility of the oxidation level of Cu oxides, promises a way to study the physics of the SOTs purely generated by the interfacial SOI.

In this Letter, we demonstrate that the intrinsic Berry-curvature mechanism is responsible for the DL SOT generation in $Ni_{81}Fe_{19}/CuO_x$ bilayers. In the bilayers where the CuO_x layer is highly oxidized and semi-insulating, we observe a sizable DL SOT in spite of the fact that the SOTs are purely generated by the interfacial SOI. We further found that the great flexibility of the oxidation level of Cu enables us to tune and even reverse the sign of the FL SOT, opening a new avenue of SOT engineering. These features are consistent with the prediction of a two-dimensional (2D) Rashba model with oxygen-modulated spin-dependent disorder.

We used the spin-torque ferromagnetic resonance (STFMR) [33–35] to quantify the SOTs in the $Ni_{81}Fe_{19}/CuO_x$ bilayers at room temperature. The bilayers were fabricated by radio frequency (rf) magnetron sputtering in

the following sequence. A 10-nm-thick CuO_x layer was first grown on a thermally oxidized Si substrate by reactive sputtering, in a mixture of argon and oxygen atmosphere of 0.25 Pa. To manipulate the oxidation level of the CuO_x layer, the oxygen to argon gas flow ratio (Q) was varied from 2.5% to 5.5%. Then, on the top of the semi-insulating CuO_x layer, a $Ni_{81}Fe_{19}$ layer with the thickness t_{FM} was grown at an argon pressure of 0.2 Pa, followed by a 4-nm-thick SiO_2 capping layer to prevent the oxidation of the $Ni_{81}Fe_{19}$ surface. The bilayers were patterned into rectangular strips with 4-μm width and 30-μm length by photolithography and liftoff techniques [see Fig. 1(a)]. For the STFMR measurement, an rf current with the frequency of f was applied along the longitudinal direction of the device, and an in-plane external field H_{ext} was applied at an angle of 45° with respect to the longitudinal direction of the device. The rf current generates the SOTs, which excite magnetic precession. The magnetization precession in the $Ni_{81}Fe_{19}$ layer causes the variation of the resistance owing to the anisotropic magnetoresistance (AMR). Therefore, the SOTs can be quantitatively determined by measuring a direct-current voltage, which is generated from the frequency mixing of the rf current and the oscillating resistance [36–38].

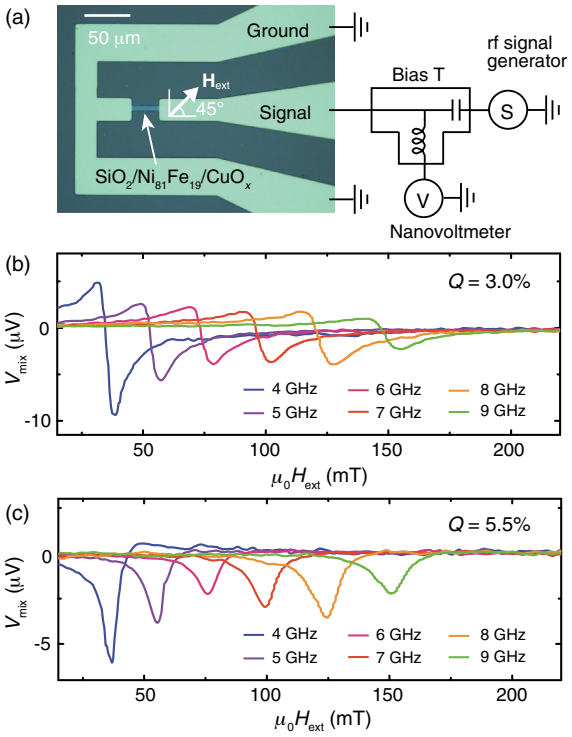

FIG. 1. (a) An optical image of the sample geometry including contact pads, with the circuit and a 45° tilt of an in-plane magnetic field $\mathbf{H}_{ext}$ with respect to the strip length direction used for the STFMR measurements. The H_{ext} dependence of the dc voltage V_{mix} for the $Ni_{81}Fe_{19}(7.5\ nm)/CuO_x$ (10 nm) bilayers with (b) $Q = 3.0\%$ and (c) 5.5% measured at the rf current frequencies of 4–9 GHz.

Figures 1(b) and 1(c) show the STFMR signals measured for the $Ni_{81}Fe_{19}/CuO_x$ bilayers with $Q = 3.0\%$ and 5.5%, respectively. The measured STFMR signals V_{mix} can be expressed as the sum of symmetric and antisymmetric Lorentzian functions [33,34]: $V_{mix} = V_s L_{sym}(H_{ext}) + V_a L_{asy}(H_{ext})$, where $L_{sym}(H_{ext}) = W^2/[(\mu_0 H_{ext} - \mu_0 H_{FMR})^2 + W^2]$ and $L_{asy}(H_{ext}) = W(\mu_0 H_{ext} - \mu_0 H_{FMR})/[(\mu_0 H_{ext} - \mu_0 H_{FMR})^2 + W^2]$. Here, W and $\mu_0 H_{FMR}$ are the linewidth and the FMR field, respectively. Figure 2(a) shows the symmetric and antisymmetric components of the measured STFMR signals, extracted by fitting the experimental data using $V_{mix} = V_s L_{sym}(H_{ext}) + V_a L_{asy}(H_{ext})$. The extracted curves demonstrate that large V_s signals are generated in both samples and the sign of V_a is opposite in the devices with $Q = 3.0\%$ and 5.5%.

The opposite sign of the antisymmetric component of the STFMR signals shows that the direction of the current-induced in-plane field in the $Ni_{81}Fe_{19}/CuO_x$ bilayers is reversed by changing the oxidation level of the CuO_x layer. In STFMR signals, the symmetric component V_s is proportional to the out-of-plane DL effective field H_{DL}, and the antisymmetric component V_a corresponds to the in-plane field $H_{\parallel}$ due to the Oersted field H_{Oe} and FL effective field H_{FL}: $H_{\parallel} = H_{Oe} + H_{FL}$ [39]. To investigate the influence of the oxidation level on the SOT generation, we summarized the Q dependence of the resistivity of CuO_x films in Fig. 2(b) and the STFMR voltage of the $Ni_{81}Fe_{19}/CuO_x$

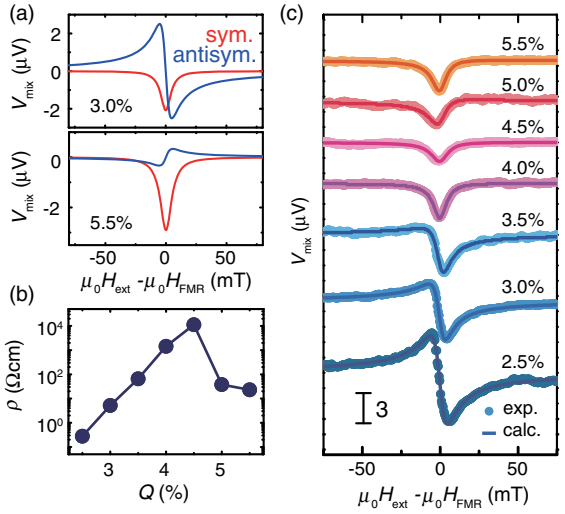

FIG. 2. (a) The fitting curves of V_{mix} as a function of the field for the $Ni_{81}Fe_{19}(7.5\ nm)/CuO_x(10\ nm)$ bilayers with $Q = 3.0\%$ and 5.5% at 7 GHz. The red and blue curves correspond to the symmetric and antisymmetric Lorentzian fitting, respectively. (b) The Q dependence of the electrical resistivity ρ of $CuO_x(10\ nm)$ single-layer films, capped with a 4-nm-thick SiO_2 protective layer. The resistivity was measured by the four-probe method. (c) The V_{mix} as a function of the field for the $Ni_{81}Fe_{19}(7.5\ nm)/CuO_x(10\ nm)$ bilayers with various Q measured at 7 GHz.

bilayers measured at 7 GHz in Fig. 2(c). It can be clearly seen that the V_s signal survives in the present entire Q range, indicating the generation of the DL SOT. On the other hand, the V_a signal, or $H_\parallel$, decreases with raising the oxidation level and even switches its sign at high Q values. The sign reversal of $H_\parallel$ is also supported by the second harmonic Hall voltage measurements for the $Ni_{81}Fe_{19}/CuO_x$ bilayers (for details, see [40]).

The DL spin-orbit effective field H_{DL} and in-plane field $H_\parallel$ in the $Ni_{81}Fe_{19}/CuO_x$ bilayers can be quantified from the STFMR signals shown in Fig. 2(c) using [6,34,46]

$$V_s = \frac{I_{rf}\Delta R}{2} H_{DL} \frac{\gamma(\mu_0 H_{FMR} + \mu_0 M_{eff})\mu_0 H_{FMR}}{2\sqrt{2}\pi f W(2\mu_0 H_{FMR} + \mu_0 M_{eff})}, \quad (1)$$

$$V_a = \frac{I_{rf}\Delta R}{2} H_\parallel \frac{(\mu_0 H_{FMR} + \mu_0 M_{eff})}{\sqrt{2} W(2\mu_0 H_{FMR} + \mu_0 M_{eff})}, \quad (2)$$

where I_{rf} is the rf current in the strip (for details, see [40]), ΔR is the AMR amplitude, γ is the gyromagnetic ratio, and $\mu_0 M_{eff}$ is the demagnetization field. In Fig. 3(a), we

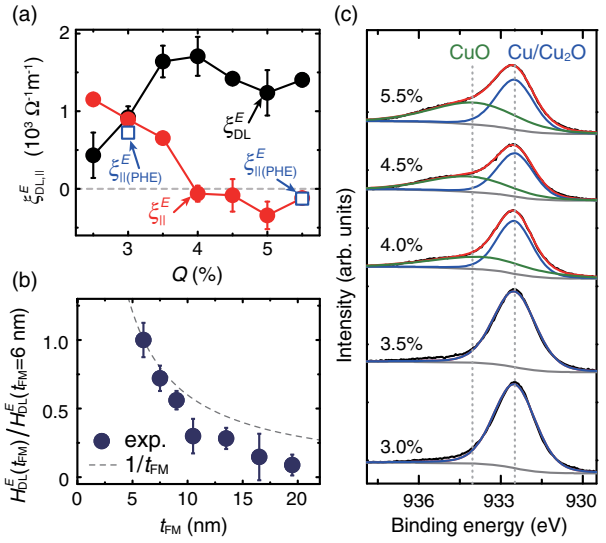

FIG. 3. (a) The estimated SOT efficiency per unit electric field $\xi^E_{DL(\parallel)}$ for the $Ni_{81}Fe_{19}(7.5\ nm)/CuO_x(10\ nm)$ bilayers with various Q values. The open squares are the in-plane torque efficiency $\xi^E_{\parallel(PHE)}$ evaluated from the second harmonic Hall voltage measurements. The red and black solid circles are $\xi^E_\parallel$ and ξ^E_{DL}, respectively, estimated from the STFMR measurements. (b) The $Ni_{81}Fe_{19}$-layer-thickness t_{FM} dependence of $H^E_{DL} = H_{DL}/E$ for the $Ni_{81}Fe_{19}(t_{FM})/CuO_x(10\ nm)$ bilayer at $Q = 3\%$, where H_{DL} is the DL spin-orbit effective field. The solid circles are the experimental data, and the dashed curve is a function proportional to $1/t_{FM}$. (c) Curves fitting Cu $2p_{3/2}$ XPS spectra for $CuO_x(10\ nm)$ single-layer films with various Q values. The red fitting curves are the merged Cu/Cu_2O (blue curves) and CuO (green curves) $2p_{3/2}$ peaks, and the gray curves are the Shirley background.

tentatively estimate the Q dependence of the torque efficiency per unit electric field E for the thickness of the FM layer $t_{FM} = 7.5$ nm, defined by [47]

$$\xi^E_{DL(\parallel)} = \frac{2e}{\hbar}\mu_0 M_s t_{FM} \frac{H_{DL(\parallel)}}{E}, \quad (3)$$

where M_s denotes the saturation magnetization. At the initial stage, ξ^E_{DL} increases nearly four times before reaching the point of $Q = 3.5\%$ and then becomes almost constant at the high oxidation level. One possible reason for the initial increase of ξ^E_{DL} can be accounted for by the enhanced Rashba parameter upon the formation of the oxide-metal interface, related to the effective electric field induced by the asymmetric charge distribution of the interface state, which is reminiscent of that observed at the Gd(0001) surface [48]. A similar enhancement of the DL SOT has also been observed in W(O)/CoFeB [49] and Pt/oxidized-CoFeB systems [50]. In contrast to the increase of ξ^E_{DL}, $\xi^E_\parallel$ decreases monotonically with increasing the Q values. The sign of $\xi^E_\parallel$ is reversed around $Q = 4\%$, quantitatively consistent with $\xi^E_{\parallel(PHE)}$ obtained from the second harmonic Hall voltage measurement.

The observed change of $\xi^E_\parallel$ originates from the sign reversal of the FL SOT induced by changing the oxidation level at the $Ni_{81}Fe_{19}/CuO_x$ interface. It is worth noting that, in the $Ni_{81}Fe_{19}/CuO_x$ bilayers, the resistivity of the CuO_x layers is more than 3 orders of magnitude higher than that of the $Ni_{81}Fe_{19}$ layer ($\sim 100\ \mu\Omega$ cm) as shown in Fig. 2(b), indicating that H_{Oe} due to current shunting through the CuO_x layer is negligible in the $Ni_{81}Fe_{19}/CuO_x$ bilayers. However, H_{Oe} can still be created by a possible nonuniform current distribution due to the different electron reflection at the top and bottom interfaces of the $Ni_{81}Fe_{19}$ layer [51]. The contribution of H_{Oe} to the observed $H_\parallel$ can be estimated by measuring the STFMR for a $Ni_{81}Fe_{19}/CuO_x$ film with thick $Ni_{81}Fe_{19}$. The reason for this is that the FL effective field H_{FL} decreases with increasing the thickness t_{FM} of the $Ni_{81}Fe_{19}$ layer, and we expect $H_{FL} \simeq 0$ and $H_\parallel \simeq H_{Oe}$ in the large t_{FM} limit. From the STFMR for the thick film, we found $H_{Oe} > 0$ for the $Ni_{81}Fe_{19}/CuO_x$ films with $Q = 3\%$ and 5.5%. Using the Fuchs-Sondheimer model [51] with the measured $H_\parallel$, we have confirmed $H_{FL} > 0$ for the $Ni_{81}Fe_{19}(7.5\ nm)/CuO_x$ film at $Q = 3.0\%$. We note that, at $Q > 4\%$, $H_\parallel = H_{FL} + H_{Oe} < 0$ as shown in Fig. 3(a). This indicates $H_{FL} < 0$ in the $Ni_{81}Fe_{19}(7.5\ nm)/CuO_x$ films with higher Q. Thus, the sign of the FL SOT is reversed from positive to negative by increasing Q (for details, see Supplemental Material [40]).

The semi-insulating feature of the CuO_x layer allows us to eliminate the generated DL SOT from the spin-transfer mechanism of the SHE, since the charge current in the CuO_x layer is negligible. Moreover, treating the interfacial SOI as a perturbation in ferromagnetic-metal–insulator

bilayers, the imagery part of the interfacial SOT, or the DL SOT, vanishes in a three-dimensional scenario regardless of any detail of a model [21]. This indicates that the extrinsic SOT is unlikely to result in the efficient generation of the DL SOT in the $Ni_{81}Fe_{19}/CuO_x$ bilayers. To further study the characteristic of the DL SOT, we measured $Ni_{81}Fe_{19}$-layer-thickness t_{FM} dependence of the DL effective field H_{DL}/E for the $Ni_{81}Fe_{19}(t_{FM})/CuO_x(10\ nm)$ bilayer at $Q = 3\%$ as shown in Fig. 3(b). The DL effective field decays faster than the $1/t_{FM}$ dependence, which is different from the $1/t_{FM}$ dependence of the SOT due to the bulk SHE [52,53].

In the $Ni_{81}Fe_{19}/CuO_x$ bilayer, both the DL and FL SOTs are generated by a SOI arising from the structural inversion symmetry breaking which is usually modeled by the Rashba SOI [54]. Since the carrier spins are exchange coupled to the magnetization in the $Ni_{81}Fe_{19}$ layer, the $Ni_{81}Fe_{19}/CuO_x$ bilayer can be approximately modeled as a 2D Rashba ferromagnet in which the itinerant spins are coupled to the localized spins via an *sd* exchange interaction with a strength of J_{ex}. In this model, the Rashba-induced DL and FL SOTs are generated by two different scattering mechanisms: (i) the FL SOT, $\boldsymbol{T}_{FL} \propto \boldsymbol{m} \times (\boldsymbol{z} \times \boldsymbol{E})$, originated from the scattering of spin carriers at the Fermi surface with a conductivitylike behavior, and (ii) the DL SOT, $\boldsymbol{T}_{DL} \propto \boldsymbol{m} \times \boldsymbol{T}_{FL}$, with an intrinsic nature arising from the Berry phase curvature in the band structure; during the acceleration of carriers induced by the applied electric field, spins tilt and generate a nonequilibrium out-of-plane spin polarization in response to an additional spin-orbit field, which gives rise to the intrinsic DL SOT [6].

In the strong exchange limit, microscopic calculations show that the FL SOT is expressed as [23]

$$\boldsymbol{T}_{FL} \sim -2e\alpha_R\nu_0\left(\frac{\varepsilon_F + J_{ex}}{\gamma_\uparrow} - \frac{\varepsilon_F - J_{ex}}{\gamma_\downarrow}\right)\boldsymbol{m} \times (\boldsymbol{z} \times \boldsymbol{E}), \quad (4)$$

where ν_0, ε_F, and $\gamma_{\uparrow(\downarrow)}$ are the density of states per spin for a 2D electron gas, the Fermi energy, and the strength of the spin-dependent disorder scattering, respectively. Equation (4) has three tunable parameters that can, in principle, explain the drastic change of the FL SOT in the $Ni_{81}Fe_{19}/CuO_x$ bilayer with the oxidation: the variation of the SOI strength α_R, the exchange strength J_{ex}, and the spin-dependent scattering rates $\gamma_{\uparrow(\downarrow)}$. First, the possible change of the Rashba SOI strength α_R at the interface induced by the oxidation cannot be responsible for the observed variation of the FL SOT. According to the theory [23], since both the DL and FL SOTs are linearly proportional to α_R, they might have the same Q dependence. This prediction is in sharp contrast to our observation shown in Fig. 3(a). Second, let us assume that the sign reversal of the FL SOT is resulted from the sign reversal of J_{ex} around $Q = 4\%$. Under this assumption, J_{ex} will be negligibly small around $Q = 4\%$. On the other hand, in this region, i.e., the weak exchange limit, the theory predicts that the DL SOT should be proportional to J_{ex}^2 while the FL SOT is still linearly proportional to the exchange energy [22]. This indicates that an abrupt decrease of ξ_{DL}^E should be observed around $Q = 4\%$. This scenario also differs from our observation of a nearly constant ξ_{DL}^E around $Q = 4\%$, and thus the change of J_{ex} is not significant in the $Ni_{81}Fe_{19}/CuO_x$ bilayer.

The origin of the observed sign change of the FL SOT induced by the oxidation can be attributed to the variation of the spin-dependent disorder scattering. Assuming a metallic limit $\varepsilon_F \gg J_{ex}$, the term in the parentheses in Eq. (4) can be simplified $\sim\varepsilon_F(1/\gamma_\uparrow - 1/\gamma_\downarrow)$. If the relative strength of the spin-dependent disorder scattering could be tuned through varying the interfacial oxidation level, it is possible to observe the sign reversal of the FL SOT without changing the sign of the DL SOT. The reason for this behavior originates from the different scattering dependence of the two components of the Rashba SOTs; the FL SOT has conductivitylike behavior and is sensitive to the spin-dependent scattering, while the intrinsic DL SOT is robust against disorders in the weak disorder regime. The sign change of the interfacial FL SOT through tuning disorders was also predicted by *ab initio* calculations for more realistic band structures [25]. For permalloy, it is demonstrated that the minority spin states of Ni at the Fermi level is heavily damped by Fe impurities due to the greatly different potentials for the two constituents [55]. Therefore, a change of $\gamma_\downarrow$ can be certainly expected if the concentration of interfacial permalloy is modulated by the interfacial oxidation level. We note that although Q was varied only slightly, from 2.5% to 5.5%, the oxidation level of the CuO_x layer is significantly changed, as evidenced in the drastic change of the resistivity ρ [see Fig. 2(b)]. As shown in Fig. 2(b), when the value of Q increases from 2.5% to 5.5%, the resistivity ρ of the CuO_x film initially increases, after approaching its highest value around $Q = 4.5\%$, and then reduces. This extraordinary tendency is because of the formation of various types of CuO_x, such as Cu_2O, CuO, or their mixture, most likely attributed to the stoichiometry-related Cu vacancies [56]. This drastic change of the oxidation state of the CuO_x layer can influence the oxidation level near the $Ni_{81}Fe_{19}/CuO_x$ interface. To further obtain information on the oxidation at the interface, the x-ray photoelectron spectra (XPS) measurements were performed on $CuO_x(10\ nm)$ single-layer films with various Q. As shown in Fig. 3(c), the CuO phase appears around $Q = 4\%$, which coincides with the oxidation level where the sign reversal of the FL SOT is observed.

In conclusion, we demonstrated that the robust intrinsic DL SOT with an interfacial feature is generated in the $Ni_{81}Fe_{19}/CuO_x$ bilayers. Although the oxidation effect on the SOT generation in metallic heterostructures has been reported previously [50], the presence of a heavy metal

layer makes it difficult to provide a physical picture of the SOT generation. In contrast, the semi-insulating feature of CuO_x enables us to reveal the physics behind the oxidation effect on the SOT generation. We noticed that the observed SOTs purely originate from the interfacial SOI in the $Ni_{81}Fe_{19}/CuO_x$ bilayers with different scattering mechanisms, i.e., the conductivitylike FL SOT and the intrinsic DL SOT, providing a basic understanding on the SOT generation. Therefore, we believe that the spin-orbit device based on Cu oxide is an ideal system for the study of the intrinsic DL SOT, as well as the interfacial oxidation-tuning SOTs.

We thank Takashi Harumoto for assistance on the Auger electron spectroscopy (AES) measurements. This work was supported by Japan Society for the Promotion of Science (JSPS) KAKENHI Grants No. 26220604 and No. 26103004, the Asahi Glass Foundation, JSPS Core-to-Core Program, and Spintronics Research Network of Japan (Spin-RNJ). H. A. acknowledges the support from the JSPS Fellowship (No. P17066). A. Q. was supported by the European Research Council via Advanced Grant No. 669442 "Insulatronics" and the Research Council of Norway through its Centres of Excellence funding scheme, Project No. 262633 "QuSpin." We also thank the referee who helped, with useful comments, to clarify the Oersted field contribution in the STFMR measurements.

*To whom all correspondence should be addressed.
ando@appi.keio.ac.jp

[1] A. Manchon, Nat. Phys. **10**, 340 (2014).
[2] T. Kuschel and G. Reiss, Nat. Nanotechnol. **10**, 22 (2015).
[3] L. Berger, Phys. Rev. B **54**, 9353 (1996).
[4] M. D. Stiles and A. Zangwill, Phys. Rev. B **66**, 014407 (2002).
[5] B. A. Bernevig and O. Vafek, Phys. Rev. B **72**, 033203 (2005).
[6] H. Kurebayashi, J. Sinova, D. Fang, A. C. Irvine, T. D. Skinner, J. Wunderlich, V. Novák, R. P. Campion, B. L. Gallagher, E. K. Vehstedt, L. P. Zârbo, K. Výborný, A. J. Ferguson, and T. Jungwirth, Nat. Nanotechnol. **9**, 211 (2014).
[7] M. I. D'yakonov and V. I. Perel, Sov. JETP Lett **13**, 467 (1971).
[8] J. E. Hirsch, Phys. Rev. Lett. **83**, 1834 (1999).
[9] S. Murakami, N. Nagaosa, and S.-C. Zhang, Science **301**, 1348 (2003).
[10] J. Sinova, D. Culcer, Q. Niu, N. A. Sinitsyn, T. Jungwirth, and A. H. MacDonald, Phys. Rev. Lett. **92**, 126603 (2004).
[11] Y. K. Kato, R. C. Myers, A. C. Gossard, and D. D. Awschalom, Science **306**, 1910 (2004).
[12] D. C. Ralph and M. D. Stiles, J. Magn. Magn. Mater. **320**, 1190 (2008).
[13] A. Brataas, A. D. Kent, and H. Ohno, Nat. Mater. **11**, 372 (2012).
[14] N. Locatelli, V. Cros, and J. Grollier, Nat. Mater. **13**, 11 (2014).
[15] V. M. Edelstein, Solid State Commun. **73**, 233 (1990).
[16] S. D. Ganichev, E. L. Ivchenko, V. V. Bel'kov, S. A. Tarasenko, M. Sollinger, D. Weiss, W. Wegscheider, and W. Prettl, Nature (London) **417**, 153 (2002).
[17] J. C. RojasSánchez, L. Vila, G. Desfonds, S. Gambarelli, J. P. Attané, J. M. D. Teresa, C. Magén, and A. Fert, Nat. Commun. **4**, 2944 (2013).
[18] A. Manchon, H. C. Koo, J. Nitta, S. M. Frolov, and R. A. Duine, Nat. Mater. **14**, 871 (2015).
[19] V. P. Amin and M. D. Stiles, Phys. Rev. B **94**, 104420 (2016).
[20] V. P. Amin and M. D. Stiles, Phys. Rev. B **94**, 104419 (2016).
[21] K.-W. Kim, K.-J. Lee, J. Sinova, H.-W. Lee, and M. D. Stiles, Phys. Rev. B **96**, 104438 (2017).
[22] H. Li, H. Gao, L. P. Zârbo, K. Výborný, X. Wang, I. Garate, F. Doğan, A. Čejchan, J. Sinova, T. Jungwirth, and A. Manchon, Phys. Rev. B **91**, 134402 (2015).
[23] A. Qaiumzadeh, R. A. Duine, and M. Titov, Phys. Rev. B **92**, 014402 (2015).
[24] J. Sinova, S. O. Valenzuela, J. Wunderlich, C. H. Back, and T. Jungwirth, Rev. Mod. Phys. **87**, 1213 (2015).
[25] F. Freimuth, S. Blügel, and Y. Mokrousov, Phys. Rev. B **90**, 174423 (2014).
[26] D. B. Buchholz, R. P. H. Chang, J.-Y. Song, and J. B. Ketterson, Appl. Phys. Lett. **87**, 082504 (2005).
[27] L. M. Huang, A. L. Rosa, and R. Ahuja, Phys. Rev. B **74**, 075206 (2006).
[28] T. S. Herng, D.-C. Qi, T. Berlijn, J. B. Yi, K. S. Yang, Y. Dai, Y. P. Feng, I. Santoso, C. Sánchez-Hanke, X. Y. Gao, A. T. S. Wee, W. Ku, J. Ding, and A. Rusydi, Phys. Rev. Lett. **105**, 207201 (2010).
[29] B. X. Yang, T. R. Thurston, J. M. Tranquada, and G. Shirane, Phys. Rev. B **39**, 4343 (1989).
[30] V. Scagnoli, U. Staub, Y. Bodenthin, R. A. de Souza, M. García-Fernández, M. Garganourakis, A. T. Boothroyd, D. Prabhakaran, and S. W. Lovesey, Science **332**, 696 (2011).
[31] K. Munakata, T. H. Geballe, and M. R. Beasley, Phys. Rev. B **84**, 161405(R) (2011).
[32] H. An, Y. Kageyama, Y. Kanno, N. Enishi, and K. Ando, Nat. Commun. **7**, 13069 (2016).
[33] L. Liu, T. Moriyama, D. C. Ralph, and R. A. Buhrman, Phys. Rev. Lett. **106**, 036601 (2011).
[34] D. Fang, H. Kurebayashi, J. Wunderlich, K. Výborný, L. P. Zârbo, R. P. Campion, A. Casiraghi, B. L. Gallagher, T. Jungwirth, and A. J. Ferguson, Nat. Nanotechnol. **6**, 413 (2011).
[35] L. Liu, C.-F. Pai, Y. Li, H. W. Tseng, D. C. Ralph, and R. A. Buhrman, Science **336**, 555 (2012).
[36] H. J. Juretschke, J. Appl. Phys. **31**, 1401 (1960).
[37] M. V. Costache, S. Watts, M. Sladkov, C. H. van der Wal, and B. J. van Wees, Appl. Phys. Lett. **89**, 232115 (2006).
[38] A. Yamaguchi, K. Motoi, A. Hirohata, H. Miyajima, Y. Miyashita, and Y. Sanada, Phys. Rev. B **78**, 104401 (2008).
[39] C.-F. Pai, Y. Ou, L. H. Vilela-Leão, D. C. Ralph, and R. A. Buhrman, Phys. Rev. B **92**, 064426 (2015).
[40] See Supplemental Material at http://link.aps.org/supplemental/10.1103/PhysRevLett.121.017202 for a detailed description of second harmonic Hall voltage measurements, determination of the rf current for STFMR

measurements, AES measurements, Oersted field due to nonuniform current distribution, and field or frequency dependence of STFMR, which includes Refs. [41–45].

[41] C. O. Avci, K. Garello, M. Gabureac, A. Ghosh, A. Fuhrer, S. F. Alvarado, and P. Gambardella, Phys. Rev. B **90**, 224427 (2014).

[42] Q. Shao, G. Yu, Y.-W. Lan, Y. Shi, M.-Y. Li, C. Zheng, X. Zhu, L.-J. Li, P. K. Amiri, and K. L. Wang, Nano Lett. **16**, 7514 (2016).

[43] Y. Wen, J. Wu, P. Li, Q. Zhang, Y. Zhao, A. Manchon, J. Q. Xiao, and X. Zhang, Phys. Rev. B **95**, 104403 (2017).

[44] E. Sondheimer, Adv. Phys. **1**, 1 (1952).

[45] M. Lucas, J. Appl. Phys. **36**, 1632 (1965).

[46] V. Tshitoyan, C. Ciccarelli, A. P. Mihai, M. Ali, A. C. Irvine, T. A. Moore, T. Jungwirth, and A. J. Ferguson, Phys. Rev. B **92**, 214406 (2015).

[47] M.-H. Nguyen, D. C. Ralph, and R. A. Buhrman, Phys. Rev. Lett. **116**, 126601 (2016).

[48] O. Krupin, G. Bihlmayer, K. Starke, S. Gorovikov, J. E. Prieto, K. Döbrich, S. Blügel, and G. Kaindl, Phys. Rev. B **71**, 201403(R) (2005).

[49] K.-U. Demasius, T. Phung, W. Zhang, B. P. Hughes, S.-H. Yang, A. Kellock, W. Han, A. Pushp, and S. S. Parkin, Nat. Commun. **7**, 10644 (2016).

[50] X. Qiu, K. Narayanapillai, Y. Wu, P. Deorani, D.-H. Yang, W.-S. Noh, J.-H. Park, K.-J. Lee, H.-W. Lee, and H. Yang, Nat. Nanotechnol. **10**, 333 (2015).

[51] A. Thiaville and Y. Nakatani, J. Appl. Phys. **104**, 093701 (2008).

[52] P. M. Haney, H.-W. Lee, K.-J. Lee, A. Manchon, and M. D. Stiles, Phys. Rev. B **87**, 174411 (2013).

[53] X. Fan, H. Celik, J. Wu, C. Ni, K.-J. Lee, V. O. Lorenz, and J. Q. Xiao, Nat. Commun. **5**, 3042 (2014).

[54] S. Grytsyuk, A. Belabbes, P. M. Haney, H.-W. Lee, K.-J. Lee, M. D. Stiles, U. Schwingenschlögl, and A. Manchon, Phys. Rev. B **93**, 174421 (2016).

[55] P. E. Mijnarends, S. Sahrakorpi, M. Lindroos, and A. Bansil, Phys. Rev. B **65**, 075106 (2002).

[56] B. K. Meyer, A. Polity, D. Reppin, M. Becker, P. Hering, P. J. Klar, T. Sander, C. Reindl, J. Benz, M. Eickhoff, C. Heiliger, M. Heinemann, J. Bläsing, A. Krost, S. Shokovets, C. Müller, and C. Ronning, Phys. Status Solidi B **249**, 1487 (2012).